Applied Materials Today 19 (2020) 100594

Contents lists available at ScienceDirect

Applied Materials Today

journal homepage: www.elsevier.com/locate/apmt

Degradation of the sporopollenin exine capsules (SECs) in human plasma

Teng-Fei Fan[a,1], Youngkyu Hwang[a,1], Michael G. Potroz[a], Kai-Lin Lau[a], Ee-Lin Tan[a], Mohammed Shahrudin Ibrahim[a], Eijiro Miyako[b], Nam-Joon Cho[a,*]

[a] School of Materials Science and Engineering, Nanyang Technological University, 50 Nanyang Avenue 639798, Singapore
[b] Department of Materials and Chemistry, Nanomaterials Research Institute (NMRI), National Institute of Advanced Industrial Science and Technology (AIST), Central 5, 1-1-1 Higashi, Tsukuba, Ibaraki 305-8565, Japan

ARTICLE INFO

Article history:
Received 2 January 2020
Received in revised form 27 January 2020
Accepted 1 February 2020

Keywords:
Pollen
Sporopollenin exine capsules
Degradation
Human plasma

ABSTRACT

The sporopollenin exine capsules (SECs) have recently attracted the attention of biological applications. The stability of SECs in human fluids is important issue to develop the controllable methods for the drug delivery system. Here, we analyzed the human plasma-triggered degradation of three species of SECs, *i.e.*, camellia (*Camellia sinensis* L.), cattail (*Typha angustifolia* L.), and dandelion (*Taraxacum officinale* L.), regarding the physical and chemical aspects. The field emission scanning electron microscopy (FESEM) images showed no significant changes in the surface morphology of the SECs as increasing incubation time in human plasma, but we observed the increase of the rupture ratio by dynamic image particle analysis (DIPA). Also, Fourier-transform infrared spectroscopy (FTIR) combined with principal component analysis (PCA) addressed the chemical degradation in a species-specific manner. Specifically, the O—H groups of camellia SECs, C—O—C groups of cattail SECs, and C=O groups of dandelion SECs showed significant changes.

1. Introduction

The pollen grains have diversity in shape, size, and complexity according to plant species [1–4]. The pollen wall structure is composed of two layers; the exine as an outer layer and intine as an inner layer [5,6]. The exine layer is mainly composed of sporopollenin that is a robust biopolymer [7]. Although its exact composition is not fully understood, the chemical-, mechanical-, and thermal-resistant properties of the sporopollenin provide potential applications as a functional biomaterial [8–12]. In particular, sporopollenin exine capsules (SECs) derived from pollen grain have been studied for micro-encapsulation [8,13–16], drug delivery [11,17–21], heavy metal binding [22], catalysis [23], and 3D scaffolds [24–26].

One particularly promising application of SECs is its use as a natural, eco-friendly, and biocompatible drug delivery agent. Previous studies have observed the potential for plant-based microcapsules in both oral delivery and injection administration applications [17,21,27]. For oral delivery, previous studies have found that sporopollenin exine capsules (SECs), *i.e.*, sporopollenin, which is the main component of microcapsule, can permeate the intestinal walls, then release their contents by the decomposition in the blood [27,28]. To produce SECs, spores or pollens were first defatted with organic solvents to remove lipidic content [8]. Alkalinolysis removes cytoplasmic components from the defatted spores, followed by a series of acetolysis, or acidic hydrolysis using hydrochloric acid, sulphuric acid, or phosphoric acid, to remove the intine layer [8,29–31]. Pollens and spores, however, have different degrees of tolerance to these commonly used but destructive processing methods. Spores and pollen can be severely damaged when placed in strong acidic or alkaline solutions. Recently, SECs extraction methods have significantly improved by using phosphoric acid processing at 70 °C, which has shown that alkaline lysis treatment is not necessary to produce SECs of equivalent quality [11,32–34]. Thus, certain pollen SECs with thin or basic-sensitive walls (e.g., corn and dandelion pollen [35]), which had been impossible to extract by conventional methods, can now be successfully extracted. These improved SECs extraction methods have opened new lines of research to investigate a wide range of previously unexplored pollen species, particularly those with thin walls that are attractive candidates for controlled drug delivery.

For biotherapeutic applications, the degradation behavior of SECs in biological environments is important. Previous studies have

* Corresponding author.
E-mail address: njcho@ntu.edu.sg (N.-J. Cho).
[1] These authors equally contributed to this work.

https://doi.org/10.1016/j.apmt.2020.100594
2352-9407/

suggested the enzyme-dependent degradation of lycopodium SECs in rat or human blood by injection or intragastric administration of drug/peptide-loaded lycopodium SECs [21,27,36,37]. However, the chemical degradation of the SECs is still not well-known.

In this study, we report the physical and chemical degradation of three species of SECs by the human plasma; camellia (Camellia sinensis L.) and cattail (Typha angustifolia L.) from dicots plant and dandelion (Taraxacum officinale L.) from monocots plants. We have previously reported the preparation and application of these pollen SECs as promising drug delivery vehicles [38,39] in terms of their size uniformity and high drug loading content. Besides, we also studied their species-specific biodegradation behavior in simulated gastrointestinal fluid [40]. Herein, to further understand the physical-chemical properties of SECs and explore their application as biomaterials, it is critical to identify their degradation behavior in human blood. Dynamic image particle analysis (DIPA) and field emission scanning electron microscopy (FESEM) show morphological characteristics of SECs such as particle size distribution, rupture ratio, and surface morphology. In addition, Fourier transform infrared spectroscopy (FTIR) confirmed SECs chemical characteristics.

2. Materials and methods

2.1. Materials

Camellia sinensis L. bee pollen was purchased from Xi'an Yuenun Biological Technology Company Ltd. (Xi'an, China). Natural *Typha angustifolia* L. pollen grains were purchased from Wong Yiu Nam Medical Hall Pte. Ltd. (Singapore). *Taraxacum officinale* L. defatted pollen grains were purchased from Greer Labs (Lenoir, NC, USA). Human plasma was purchased from Axil Scientific Pte Ltd. (Singapore). Blood cells were removed by centrifugation at 2000*g* for 15 min. Simulated body fluid (SBF) was prepared via previously described methods [41]. All chemical reagents were purchased from Sigma-Aldrich (St. Louis, MD, USA) as described in the Supplementary Information.

2.2. SECs extraction

Camellia, cattail, and dandelion SECs were prepared via previously reported methods [32,33], with slight modifications.

Camellia SECs: First, 250 g of camellia bee pollen was refluxed in acetone (500 mL, 50 °C) under stirring (220 rpm) for 3 h. The supernatant was then decanted, and pollen was washed with 1 L of warm water (50 °C) under stirring until the bee pollen aggregates were disintegrated into individual particles. The contaminants, such as plant/animal tissues were removed by a nylon mesh (150 μm in pore size, ELKO Filtering Co. LLC, Miami, FL, USA). Pollen particles were collected from the filtrate via vacuum filtration, and this washing step was repeated twice.

The resulting pollen was refluxed in acetone again and then dried in a glass dish. Dried pollen (20 g) was further washed by diethyl ether (250 mL) under stirring (300 rpm) for 2 h at room temperature. This washing step was repeated twice. After that, the pollen was resuspended in diethyl ether (500 mL) overnight under constant stirring (300 rpm). The pollen was collected using vacuum filtration and dried in a fume hood.

The defatted pollen (10 g) was refluxed (70 °C, 220 rpm) in 85% (v/v) phosphoric acid (100 mL) for 5 h. SECs were filtered and washed by the following solvents (50 mL): water (5 times), acetone (2 times), 2 M hydrochloric acid (1 time), 2 M sodium hydroxide (1 time), water (5 times), acetone (1 time), ethanol (2 time), and water (1 time). SECs were dried overnight in a vacuum oven (60 °C).

Cattail SECs: Natural cattail pollen (10 g) were refluxed in acetone (45 °C, 200 rpm) for 30 min. Pollen grains were collected by vacuum filtration and washed with acetone (50 mL) again. The defatted pollen was obtained after drying at room temperature.

Defatted pollen grains (2 g) were refluxed (70 °C, 200 rpm) in 85% (v/v) phosphoric acid (15 mL) for 2.5 h. The contents were then cooled to room temperature before dilution with deionized water (150 mL) and vacuum filtration. SECs were collected and washed with warm water (150 mL). The water wash was repeated until the pH of pollen solution achieved 6–7. Resulting SECs were collected and washed via consecutive rinsing with the following solvents (100 mL, 50 °C): acetone (2 times), 2 M hydrochloric acid (1 time), 2 M sodium hydroxide (1 time), water (5 times), acetone (1 time), ethanol (2 times), and a final water wash (3 times). During each wash, SECs were continuously stirred in a beaker to prevent clumping. The solvent was then removed by vacuum filtration. SECs were then collected and dried in a vacuum oven (60 °C).

Dandelion SECs: Similarly, defatted dandelion pollen (2 g) was also refluxed (70 °C, 200 rpm) in 85% (v/v) phosphoric acid (15 mL) for 5 h. Then, SECs were washed by the following solvents (100 mL, 50 °C): water (5 times), acetone (2 times), 2 M hydrochloric acid (1 time), 2 M sodium hydroxide (1 time), water (5 times), acetone (1 time), ethanol (2 times), and water (1 time). The SECs were collected using vacuum filtration and dried in a vacuum oven (60 °C, 4 h).

2.3. SECs human plasma treatment

For each pollen species, 120 mg of SECs was split into three batches (40 mg per batch). Two batches were suspended into human plasma (0.6 mL), mixed by vortex (1 min), and incubated at 37 °C for 1 h and 48 h, separately, using orbital shaker incubator (220 rpm, LM-450D, Yihder, New Taipei City, Taiwan). The third batch was used as the control group and incubated with deionized water (0.6 mL) using the same incubation conditions. Subsequently, the respective SECs were collected at specific time points (1 h and 48 h) via centrifugation (7000 rpm, 15 min), and consecutively washed with SBF (5 × 1 mL) and deionized water (5 × 1 mL), and then lyophilized.

2.4. Dynamic image particle analysis (DIPA)

DIPA was performed in a FlowCAM benchtop system FlowCamVS, Fluid Imaging Technologies, Scarborough, ME, USA, which was equipped with a flow cell 200 μm, FC-200 and a lens 20× magnification, Olympus, Tokyo, Japan. SECs samples were diluted in deionized water with a concentration of 2 mg/mL, then loaded into the flow cell and analyzed at a flow rate of 0.1 mL/min. The camera rate was set at 14 frames per second. Over 5000 particles were counted for each measurement with triplicate for each sample. 500 Well-focused SECs particles were sampled by edge gradient ordering and manual processing. Before the measurement, standard polystyrene microspheres 50 ± 1 μm were used to calibrate the instrument.

2.5. Fourier-transform infrared spectroscopy (FTIR) spectroscopy

FTIR was conducted using a diamond cell attenuated total reflection accessory (PerkinElmer Spectrum, Seer Green, Buckinghamshire, UK). Reflectance infrared spectra were obtained between 4000 cm^{-1} and 600 cm^{-1} by 16 times scanning per measurement and 6 repeats per sample.

Background spectra were collected prior to sample readings and subtracted from each spectrum automatically. Baseline corrections were made using the Spectrum 10 software (Seer Green, Buckinghamshire, UK). Each spectrum was standardized according to previously described methods [42]. Briefly, we used the formula; $(x–x–)/\sigma$, where x refers to the absorbance value, x– to the spectrum arithmetic mean, and σ to the spectrum standard devia-

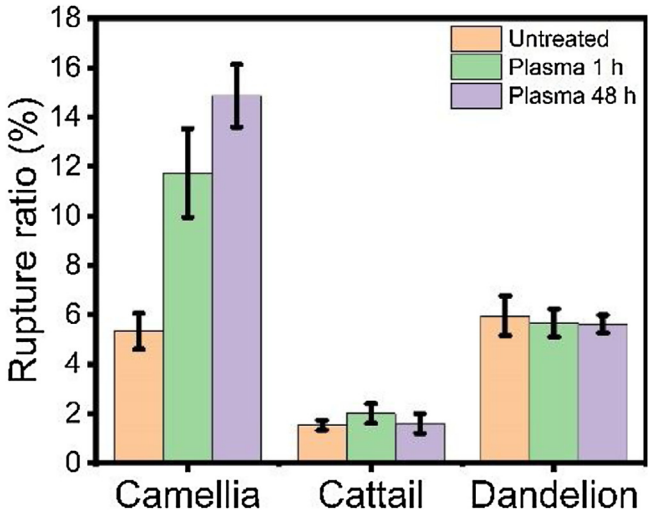

Fig. 1. Results of the DIPA analysis for camellia, cattail, and dandelion SECs before and after human plasma treatment. The rupture ratio of each sample was calculated based on the Flowcam images of 500 pollen particles. The data represented the average of triplicate measurements for each sample with standard deviations indicated by error bars.

tion. Peak heights were obtained by gathering the maximum value within a range (Table 2). Peak height ratios between target peaks and referrer peaks were calculated to remove sample thickness effects for the absolute absorbance values. Principal component analysis (PCA) on the FTIR spectra was conducted using the Origin 2018 software (OriginLab, USA).

2.6. Field emission scanning electron microscopy (FESEM)

Surface morphological characterization of SECs was performed by a FESEM JSM-7600 F (JEOL, Tokyo, Japan) at a 5.00 kV acceleration voltage under various magnifications (2500×, 15,000×, and 20,000×). All untreated and human plasma-treated SECs samples were lyophilized in a freeze dryer (Labconco, Kansas City, MO, USA) for 2 days. Samples prepared for imaging were spread onto conductive carbon tapes and coated with gold (thickness = 20 nm) using a JFC-1600 Auto Fine Coater (20 mA, 80 s, JEOL, Japan). Visual inspection of n > 50 of SECs particles from the untreated and human plasma-treated was conducted to analyze morphological changes.

2.7. Statistical analysis

In this study, quantitative data are presented as the mean ± standard deviation (SD). The statistical analysis was performed using ANOVA (Single factor) method. A p-value of <0.05 was considered statistically significant.

3. Results and discussion

3.1. Physical characterization of the SECs samples

3.1.1. DIPA measurements of the SECs samples

The results of the DIPA measurements are presented in Fig. 1 and Table 1. The aspect ratio, diameter, and circularity for the broken particle population and morphological parameters were measured to characterize physical SECs degradation (Table 1). The representative intact SECs were imaged at various angles, where we defined broken particles as particles characterized by cracks, holes, and fragmentations (Fig. S1). Although the morphological parameters for the three SECs species had no significant differences in terms

Table 1
Morphological parameters for the three pollen SECs species before and after human plasma treatment.

Species	Treatment	Aspect ratio	Diameter (μm)	Circularity
Camellia	Untreated	0.87 ± 0.09	32.22 ± 3.39	0.97 ± 0.05
	Plasma 1 h	0.86 ± 0.08	32.13 ± 3.12	0.97 ± 0.04
	Plasma 48 h	0.85 ± 0.09	32.73 ± 3.86	0.97 ± 0.05
Cattail	Untreated	0.80 ± 0.11	19.52 ± 2.15	0.95 ± 0.06
	Plasma 1 h	0.83 ± 0.09	19.21 ± 1.43	0.97 ± 0.03
	Plasma 48 h	0.83 ± 0.10	19.49 ± 1.67	0.96 ± 0.04
Dandelion	Untreated	0.88 ± 0.11	27.11 ± 5.14	0.97 ± 0.06
	Plasma 1 h	0.90 ± 0.09	27.96 ± 3.44	0.98 ± 0.04
	Plasma 48 h	0.89 ± 0.08	28.10 ± 3.63	0.98 ± 0.04

of aspect ratio, diameter, and circularity before and after human plasma incubation treatment (Table 1), we observed broken particles after visual inspection of each single particle. Interestingly, the rupture ratio suggests the presence of a species-dependent degradation behavior. As it was shown in Fig. 1, Camellia SECs exhibited the most degradation with a ~2.8-fold increase in the broken particle population after incubation in human plasma for 48 h (from 5.32 ± 0.73 to 14.9 ± 1.27%). However, cattail and dandelion SECs had no significant difference in their broken particle population.

3.1.2. Surface morphology characterization of the SECs samples

We further characterized SECs surface morphology to evaluate the presence of surface degradation on the treated SECs. Similar to our previous studies [21,27,36], FESEM shows that no significant surface degradation occurred on the SECs after human plasma treatment (Fig. 2). Each species of SECs still kept their unique microstructure after human plasma treatment for 48 h. Typically, Camellia SECs are triaperturate, with three cleavage planes (Fig. 2A). Cattail SECs are monopartite with net-shaped surface (Fig. 2B), dandelion SECs possess three endoapertures that are surrounded by ridges (Fig. 2C). Furthermore, intact exine layer (Fig. 2) in each the SECs species was also observed, which showing no morphology difference between untreated samples and human plasma treated samples

3.2. Chemical characterization of the SECs samples

3.2.1. FTIR spectra of the SECs samples

FTIR spectra for the untreated and treated SECs were also collected to investigate their respective chemical composition (Fig. 3) [43]. On the basis of previous studies of pollen, sporopollenin, and sporoderm, major FTIR peaks were assigned functional groups as presented in Table 2. The spectra for the different species were similar from 2800 to 3500 cm^{-1}, with the majority of variation occurring from 700 to 1700 cm^{-1}. Although C=O (about 1680 cm^{-1}) and C—O—C peaks (about 1100 cm^{-1}) exist in the spectra for all three species, the C=O peak was stronger for camellia SECs, whereas the C—O—C peaks were stronger for the cattail and dandelion SECs. Furthermore, aromatic groups (800–900 cm^{-1}) had strong absorbance in camellia and cattail, but less so for dandelion. Overall, these results confirm the presence of a species-dependent SECs composition, which is in agreement with previous studies that have shown that sporopollenin is composed of phenolic and polyhydroxylated aliphatics that are covalently coupled by ether and ester bonds [6,44].

Difference absorbance spectra were obtained by subtracting the mean untreated SECs spectra from the spectra after human plasma treatment to highlight spectral changes during SECs incubation with human plasma (Fig. 4). The spectra for all three SECs species exhibited a small decrease in C—H peaks at 2850 and 2926 cm^{-1} after human plasma treatment, which suggests that the —CH_3 and

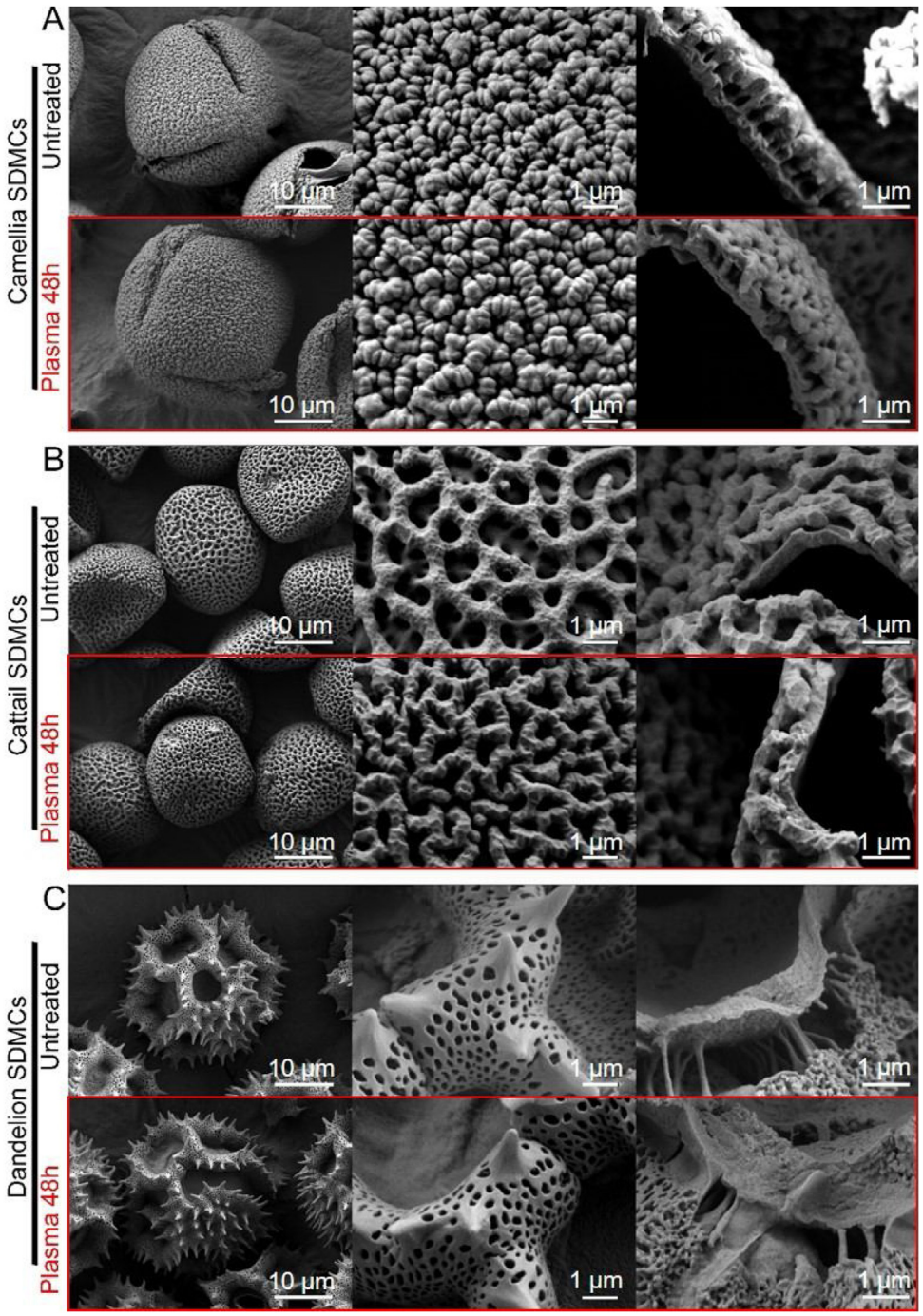

Fig. 2. FESEM images of camellia, cattail, and dandelion SECs before and after human plasma treatment. (A) Camellia SECs, (B) cattail SECs, and (C) dandelion SECs. Single PMC particle, microstructure, and cross-section perspectives were photographed at various magnifications. Scale bar (from left to right) represents 10 μm, 1 μm, and 1 μm.

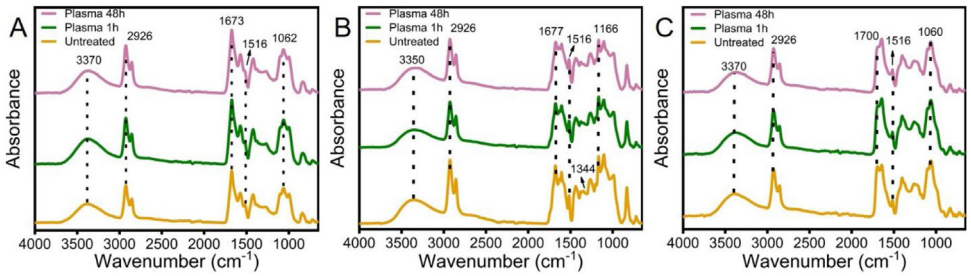

Fig. 3. The standardized mean FTIR spectra for untreated SECs and SECs after human plasma treatment (n = 6). (A) camellia SECs, (B) cattail SECs, and (C) dandelion SECs.

Table 2
Peak assignments for absorbance peaks in the SECs FTIR spectra [42,43,45].

Wavenumber (cm^{-1})	Assignment	Interpretation
3370 (camellia and dandelion), 3350 (cattail)	νO—H	Hydroxyl
2926	ν_{as} CH_2	Aliphatic
1673 (camellia), 1677 (cattail), 1696 (dandelion)	νC=O	Ester groups
1516	νC=C	Aromatic compounds
1062 (camellia), 1104 (cattail), 1060 (dandelion)	νC—O—R	Carbohydrate

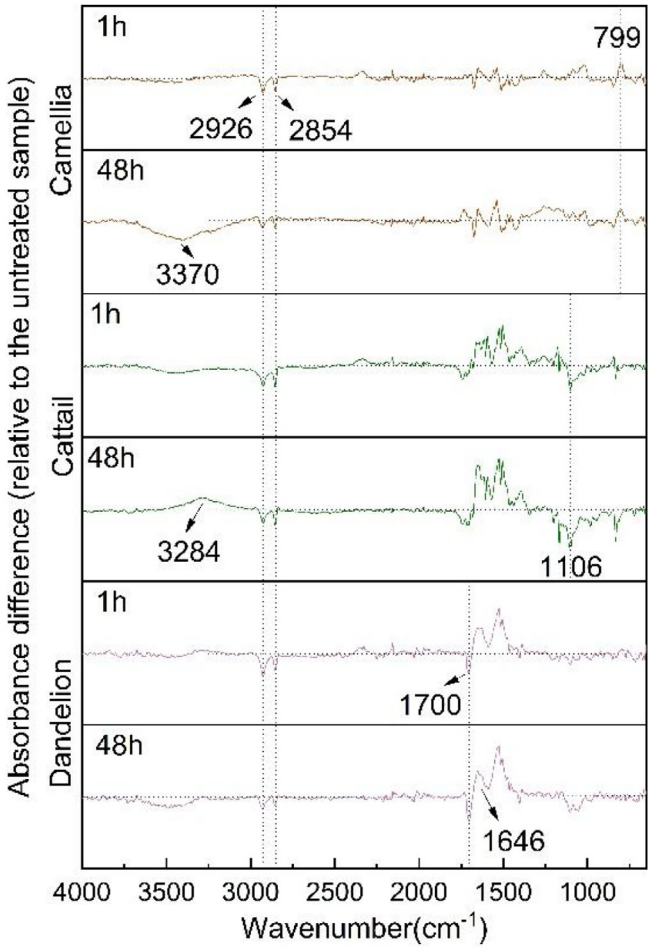

Fig. 4. FTIR absorbance difference spectra for camellia SECs (camellia), cattail SECs (cattail), and dandelion SECs (dandelion) SECs after degradation treatment for 1 h and 48 h. The subtraction of the mean spectra for untreated SECs from the human plasma-treated sample mean spectrum yielded each spectrum. Dashed lines indicate the 0 value.

—CH_2 groups degraded. In addition, the majority of spectral changes were observed from 700 to 1700 cm^{-1}, which is in agreement with previous studies and is related to new bond formation, such as C=C and C—O—C bonds.

For camellia SECs, the most significant decrease in peak intensity occurred at O—H vibrations (3370 cm^{-1}) after human plasma treatment for 48 h, which indicates the breakdown of O—H bonds in the SECs. Peak fluctuation is also observed from 700 to 1700 cm^{-1}, although there was no clear trend as incubation time increased from 1 to 48 h. For cattail SECs, the O—H vibration peak (about 3350 cm^{-1}) decreased after 1 h of incubation in human plasma but increased from 3350 to 3284 cm^{-1} after 48 h of incubation in human plasma, which indicated newly formed O—H bonds. The most significant decrease in peak intensity occurred for C—O—C vibrations (1106 cm^{-1}). For dandelion SECs, a sharp decrease in the C=O peak (1700 cm^{-1}) with a substantial increase in the C=C peak (1646 cm^{-1}) suggests carboxyl group degradation and carbon-carbon double bond formation.

3.2.2. Analysis of peak height ratios

Peak height ratios were calculated to compare peak changes related to specific functional groups (Fig. 5). Peaks at 1573 cm^{-1}, 1344 cm^{-1}, and 832 cm^{-1} were chosen as internal peak references for camellia, cattail, and dandelion, respectively, as they were characterized by the least amount of change in degradation during incubation in human plasma.

Normalized peak height ratio variations for human plasma treated samples were subsequently summarized in Fig. 6. We observed the most significant increase in peak height ratio (1.42) in dandelion SECs, which correlates with C=C bonds. Given the knowledge that polysaturated fatty acid metabolizes in mammals through desaturation, we infer that a similar mechanism was involved with dandelion SECs degradation in human blood. The most significant decrease was observed for camellia SECs, which correlates with O—H bonds (Figs. 4 and 6). After 48 h treatment in human plasma, the peak ratio of camellia SECs O—H bonds decrease to 0.89 (Fig. 6). Our results suggest that hydroxyl groups were the main contributing factor to camellia SECs degradation in human plasma.

Overall, each functional group exhibited different trends in peak height ratio for the three SECs species. Although the O—H ratio decreased after 48 h of incubation in human plasma for camellia, it increased in cattail and did not change in dandelion. Furthermore, the C=C peak height ratio increased for cattail and dandelion SECs after 48 h of incubation in human plasma but decreased for camellia SECs. In general, these results indicate how different SECs may degrade through species-specific pathways in human plasma.

3.2.3. Principal component analysis (PCA)

In order to compare the whole spectra and to cluster samples based on the spectral properties, we performed principal component analysis (PCA) on the FTIR spectra of untreated and human plasma treated SECs samples for each pollen species, separately (Fig. 7). This method is extensively used in the interpretation of FTIR spectra, which includes various chemical changes. PCA was performed at regions between 2000 and 600 cm^{-1} (Fig. 7A–C), and for the entire spectral data set (4000 to 600 cm^{-1}, Fig. 7D–F). The results were plotted on the basis of the first and second PC, which contributed to more than 90% of the spectral variation.

PCA for camellia and cattail SECs (Figs. 7A, B, D, E) show that the spectral characteristics of the degraded samples are separable from untreated controls, which means that the polymer composition of the human plasma-incubated camellia and cattail SECs is changed. To better understand the chemical bonds that mainly contribute to the spectral differences, the loading of the given two principal components in partial and whole spectra data was plotted in Fig. S2. Based on the loading plots, we infer that the O—H, C—H, and C=O groups in camellia contributed the most toward spectral differences. For cattail, peaks in the fingerprint region (900–1300 cm^{-1}) were characterized by a strong decrease, which may be associated with C—O—C bonds (Fig. S2).

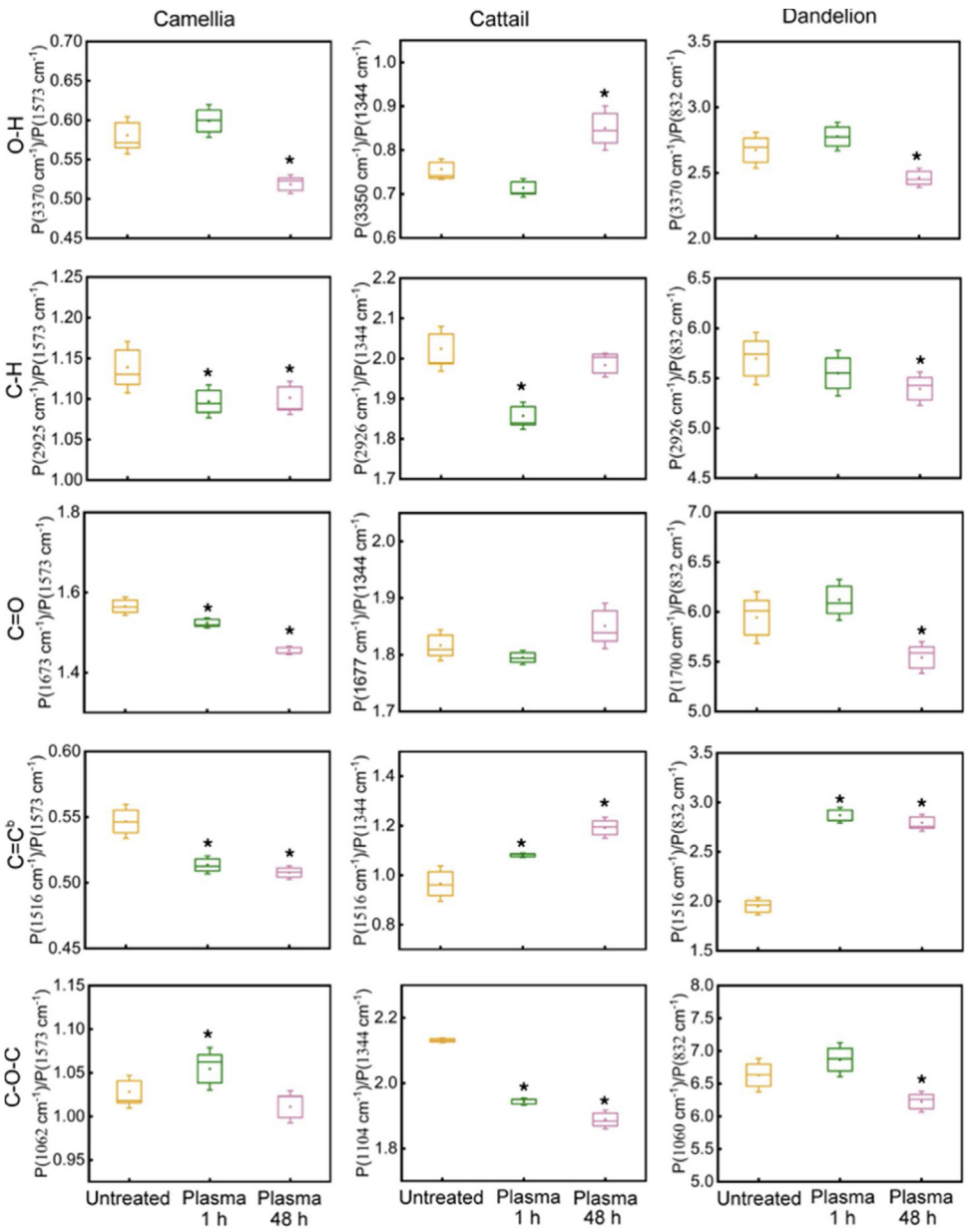

Fig. 5. Box plots represent calculated peak height ratios of functional group (O—H, C—H, C=O, C=C, and C—O—C) for the untreated SECs (yellow) and human plasma treated SECs for 1 h (green) and 48 h (purple). Internal standard peaks were set at 1573 (camellia), 1344 (cattail), and 832 cm^{-1} (dandelion). The line and dot in the box indicate median and the mean value. The whiskers indicate the minimum and maximum values, S.D., *P < 0.05.

Full-spectrum analysis of dandelion SECs shows overlapped region in human plasma treated and untreated SECs (Fig. 7F). In comparison, analyses in 2000 to 600 cm^{-1} (Fig. 7C) reveals a clear separation, which suggests that major spectra variations occurred in this range. Although PC2 only contributed 3.0% of the variation, it appears to play a dominant role in sample spread. On the basis of the loading plot (Fig. S1), the increased peak at 1696 cm^{-1} induced separation in the PC2 *Y* axis. This is in agreement with previous results that we observed in the FTIR spectra and peak height ratio variation, where the C=O and C=C peaks were characterized by significant variation.

4. Conclusions

We investigated the degradation behavior of three SECs species, *i.e.*, *Camellia sinensis* L. (camellia), *Typha angustifolia* L. (cattail), and *Taraxacum officinale* L. (dandelion), in human plasma. Morphological changes were characterized via FESEM and DIPA, and changes in chemical composition were characterized by FTIR spectroscopy and analyzed via PCA. Although there is no significant change in the surface morphology of the SECs as increasing incubation time in human plasma, we observed the increase of the rupture ratio induced by the crack at the edge of the aperture. In addition, FTIR spectroscopy and PCA addressed that each SECs show composition changes in the different functional groups; the decrease of O—H groups in camellia SECs, increase of C—O—C groups in cattail SECs, and increase of C=O groups in dandelion SECs. We showed the physical and chemical degradation behavior of SECs in a species-dependent manner by the physiological environments. Taken together, this study provides fundamental information to widen the usage of the pollen-based microcapsules for biological applications. Potentially control release profiles can

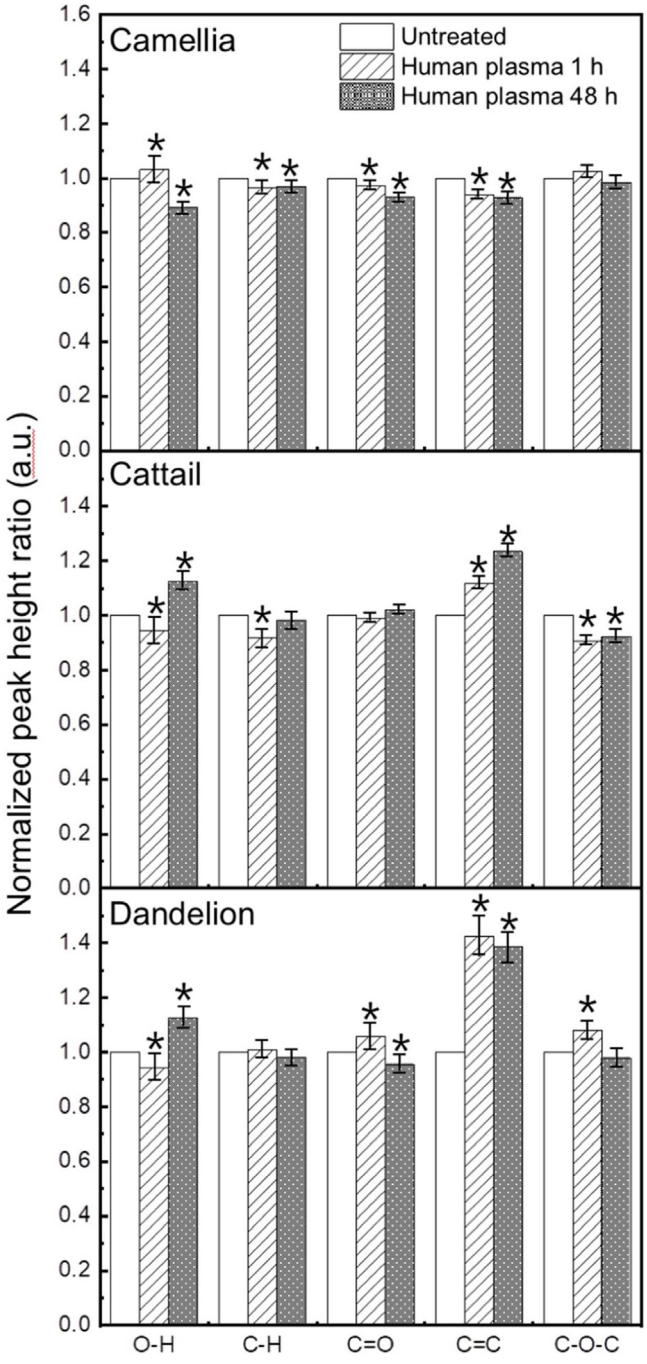

Fig. 6. Normalized peak height ratio for SECs before and after human plasma treatment. As the internal reference, the peak ratio of the target functional groups from untreated samples was set to 1. The peak ratio was the mean value of six replicates, *P < 0.05.

be drawn depending on the choice and preparation of pollen. Fast degradation can contribute to remove the particles in the blood after the short-term usage; on the other hand, the pollen particle with slow degradation can retain the function as the drug carrier for a chronic disease which requires the long-term drug release.

Declaration of interests

The authors declare that they have no known competing financial interests or personal relationships that could have appeared to influence the work reported in this paper.

Data availability

All the data supporting the findings of this study are available from the corresponding authors upon reasonable request.

Acknowledgments

This work was supported by the Competitive Research Programme (NRF-CRP10-2012-07) at the National Research Foundation of Singapore (NRF) and by the Creative Materials Discovery Program through the National Research Foundation of Korea (NRF) funded by the Ministry of Science, ICT, and Future Planning

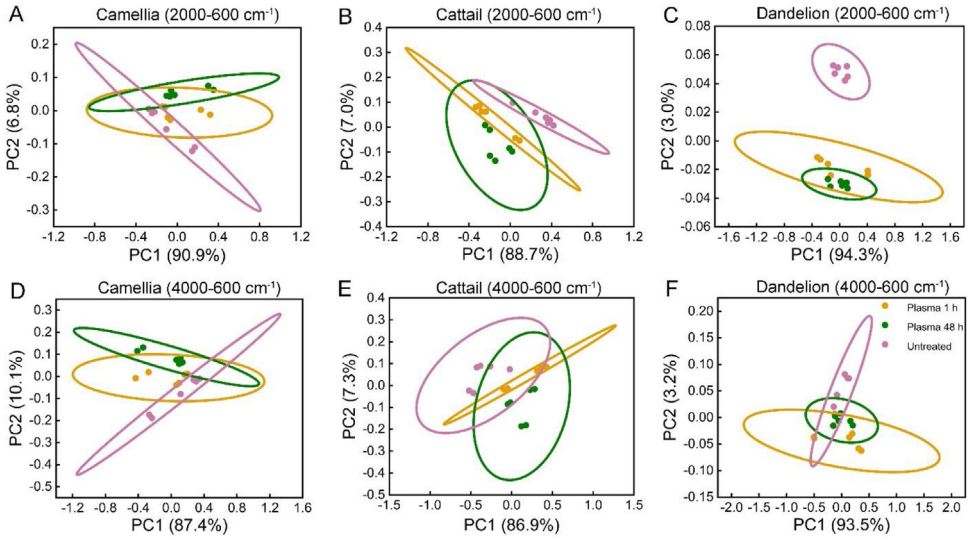

Fig. 7. FTIR spectra PCA for camellia, cattail, and dandelion SECs. PCA for the range between 2000 and 600 cm^{-1}: (A) camellia SECs, (B) cattail SECs, and (C) dandelion SECs. PCA for the full spectra: (D) camellia SECs, (E) cattail SECs, and (F) dandelion SECs. Green dots denote untreated controls; black dots indicate a 1 h sample treatment with human plasma, and red dots denote a 48 h sample treatment with human plasma. Ellipses represent 95% confidence intervals for each group.

(2016M3D1A1024098). The research also benefited from aid from a Start-Up Grant (SUG) from the Nanyang Technological University (M4080751.070). Also, this work was also supported by a Japan Society for the Promotion of Science (JSPS) KAKENHI Grant-in-Aid for Scientific Research (B) (no. 16H03834) and the JSPS KAKENHI Fund for the Promotion of Joint International Research (Fostering Joint International Research) (no. 16KK0117).

Appendix A. Supplementary data

Supplementary material related to this article can be found, in the online version, at https://doi.org/10.1016/j.apmt.2020.100594.

References

[1] A. Matamoro-Vidal, C. Prieu, C.A. Furness, B. Albert, P.H. Gouyon, Evolutionary stasis in pollen morphogenesis due to natural selection, New Phytol. 209 (1) (2016) 376–394.
[2] N.I. Gabarayeva, Pollen wall and tapetum development in Anaxagorea brevipes (Annonaceae): sporoderm substructure, cytoskeleton, sporopollenin precursor particles, and the endexine problem, Rev. Palaeobot. Palynol. 85 (3–4) (1995) 123–152.
[3] H. Linskens, Pollen physiology, Annu. Rev. Plant Physiol. 15 (1) (1964) 255–270.
[4] B. Albert, A. Ressayre, C. Dillmann, A.L. Carlson, R.J. Swanson, P.-H. Gouyon, A.A. Dobritsa, Effect of aperture number on pollen germination, survival and reproductive success in Arabidopsis thaliana, Ann. Bot. (2018).
[5] E. Katifori, S. Alben, E. Cerda, D.R. Nelson, J. Dumais, Foldable structures and the natural design of pollen grains, Proc. Natl. Acad. Sci. 107 (17) (2010) 7635–7639.
[6] T.D. Quilichini, E. Grienenberger, C.J. Douglas, The biosynthesis, composition and assembly of the outer pollen wall: a tough case to crack, Phytochemistry 113 (2015) 170–182.
[7] R. Wiermann, S. Gubatz, Pollen Wall and Sporopollenin, International Review of Cytology, Elsevier, 1992, pp. 35–72.
[8] S. Barrier, Physical and Chemical Properties of Sporopollenin Exine Particles, University of Hull, 2008.
[9] H. Lin, Z. Qu, J.C. Meredith, Pressure sensitive microparticle adhesion through biomimicry of the pollen–stigma interaction, Soft Matter 12 (11) (2016) 2965–2975.
[10] O.O. Fadiran, J.C. Meredith, Surface treated pollen performance as a renewable reinforcing filler for poly (vinyl acetate), J. Mater. Chem. A 2 (40) (2014) 17031–17040.
[11] M.G. Potroz, R.C. Mundargi, J.J. Gillissen, E.L. Tan, S. Meker, J.H. Park, H. Jung, S. Park, D. Cho, S.I. Bang, Plant-based hollow microcapsules for oral delivery applications: toward optimized loading and controlled release, Adv. Funct. Mater. 27 (31) (2017).
[12] G. Mackenzie, A.N. Boa, A. Diego-Taboada, S.L. Atkin, T. Sathyapalan, Sporopollenin, the least known yet toughest natural biopolymer, Front. Mater. 2 (2015) 66.
[13] S. Barrier, A. Diego-Taboada, M.J. Thomasson, L. Madden, J.C. Pointon, J.D. Wadhawan, S.T. Beckett, S.L. Atkin, G. Mackenzie, Viability of plant spore exine capsules for microencapsulation, J. Mater. Chem. 21 (4) (2011) 975–981.
[14] S. Barrier, A.S. Rigby, A. Diego-Taboada, M.J. Thomasson, G. Mackenzie, S.L. Atkin, Sporopollenin exines: a novel natural taste masking material, LWT-Food Sci. Technol. 43 (1) (2010) 73–76.
[15] A. Diego-Taboada, P. Cousson, E. Raynaud, Y. Huang, M. Lorch, B.P. Binks, Y. Queneau, A.N. Boa, S.L. Atkin, S.T. Beckett, Sequestration of edible oil from emulsions using new single and double layered microcapsules from plant spores, J. Mater. Chem. 22 (19) (2012) 9767–9773.
[16] R.C. Mundargi, M.G. Potroz, S. Park, H. Shirahama, J.H. Lee, J. Seo, N.J. Cho, Natural sunflower pollen as a drug delivery vehicle, Small 12 (9) (2016) 1167–1173.
[17] A. Diego-Taboada, S.T. Beckett, S.L. Atkin, G. Mackenzie, Hollow pollen shells to enhance drug delivery, Pharmaceutics 6 (1) (2014) 80–96.
[18] M.J. Uddin, H.S. Gill, Ragweed pollen as an oral vaccine delivery system: mechanistic insights, J. Control. Release 268 (2017) 416–426.
[19] S.U. Atwe, Y. Ma, H.S. Gill, Pollen grains for oral vaccination, J. Control. Release 194 (2014) 45–52.
[20] S.M. Alshehri, H.A. Al-Lohedan, A.A. Chaudhary, E. Al-Farraj, N. Alhokbany, Z. Issa, S. Alhousine, T. Ahamad, Delivery of ibuprofen by natural macroporous sporopollenin exine capsules extracted from Phoenix dactylifera L, Eur. J. Pharm. Sci. 88 (2016) 158–165.
[21] N. Sudareva, O. Suvorova, N. Saprykina, A. Vilesov, P. Bel'tiukov, S. Petunov, A. Radilov, Two-level delivery systems for oral administration of peptides and proteins based on spore capsules of Lycopodium clavatum, J. Mater. Chem. B 5 (37) (2017) 7711–7720.
[22] N. Ünlü, M. Ersoz, Adsorption characteristics of heavy metal ions onto a low cost biopolymeric sorbent from aqueous solutions, J. Hazard. Mater. 136 (2) (2006) 272–280.
[23] T. Baran, I. Sargin, M. Kaya, A. Menteş, T. Ceter, Design and application of sporopollenin microcapsule supported palladium catalyst: remarkably high turnover frequency and reusability in catalysis of biaryls, J. Colloid Interface Sci. 486 (2017) 194–203.
[24] D.A. Erdogan, T. Solouki, E. Ozensoy, A versatile bio-inspired material platform for catalytic applications: micron-sized “buckyball-shaped” TiO 2 structures, RSC Adv. 5 (58) (2015) 47174–47182.
[25] L. Wei, K. Tian, X. Zhang, Y. Jin, T. Shi, X. Guo, 3D Porous hierarchical microspheres of activated carbon from nature through nanotechnology for electrochemical double-layer capacitors, ACS Sustain. Chem. Eng. 4 (12) (2016) 6463–6472.
[26] L. Wang, J.A. Jackman, E.-L. Tan, J.H. Park, M.G. Potroz, E.T. Hwang, N.-J. Cho, High-performance, flexible electronic skin sensor incorporating natural microcapsule actuators, Nano Energy 36 (2017) 38–45.
[27] L.J. Blackwell, Sporopollenin Exines As a Novel Drug Delivery System, University of Hull, 2007.
[28] V.N. Paunov, G. Mackenzie, S.D. Stoyanov, Sporopollenin micro-reactors for in-situ preparation, encapsulation and targeted delivery of active components, J. Mater. Chem. 17 (7) (2007) 609–612.
[29] F. Zetzsche, P. Kalt, J. Liechti, E. Ziegler, Zur Konstitution des Lycopodium-Sporonins, des Tasmanins und des Lange-Sporonins. XI. Mitteilung über die Membran der Sporen und Pollen, Adv. Synth. Catal. 148 (9–10) (1937) 267–286.

[30] F. Zetzsche, O. Kälin, Untersuchungen über die membran der sporen und pollen V. 4. Zur autoxydation der sporopollenine, Helv. Chim. Acta 14 (1) (1931) 517–519.
[31] F. Zetzsche, K. Huggler, Untersuchungen über die Membran der Sporen und pollen. I. 1. Lycopodium clavatum l, Justus Liebigs Ann. Chem. 461 (1) (1928) 89–109.
[32] M.K. Corliss, C.K. Bok, J. Gillissen, M.G. Potroz, H. Jung, E.-L. Tan, R.C. Mundargi, N.-J. Cho, Preserving the inflated structure of lyophilized sporopollenin exine capsules with polyethylene glycol osmolyte, J. Ind. Eng. Chem. (2017).
[33] R.C. Mundargi, M.G. Potroz, J.H. Park, J. Seo, E.-L. Tan, J.H. Lee, N.-J. Cho, Eco-friendly streamlined process for sporopollenin exine capsule extraction, Sci. Rep. 6 (2016).
[34] J.H. Park, J. Seo, J.A. Jackman, N.-J. Cho, Inflated sporopollenin exine capsules obtained from thin-walled pollen, Sci. Rep. 6 (2016) 28017.
[35] T. Fan, J.H. Park, Q.A. Pham, E.-L. Tan, R.C. Mundargi, M.G. Potroz, H. Jung, N.-J. Cho, Extraction of cage-like sporopollenin exine capsules from dandelion pollen grains, Sci. Rep. 8 (1) (2018) 6565.
[36] M. Lorch, M.J. Thomasson, A. Diego-Taboada, S. Barrier, S.L. Atkin, G. Mackenzie, S.J. Archibald, MRI contrast agent delivery using spore capsules: controlled release in blood plasma, Chem. Commun. (42) (2009) 6442–6444.
[37] T.-F. Fan, M.G. Potroz, E.-L. Tan, J.H. Park, E. Miyako, N.-J. Cho, Human blood plasma catalyses the degradation of Lycopodium plant sporoderm microcapsules, Sci. Rep. 9 (1) (2019) 2944.
[38] E.-L. Tan, M.G. Potroz, G. Ferracci, J.A. Jackman, H. Jung, L. Wang, N.-J. Cho, Functionalized natural particles: light-induced surface modification of natural plant microparticles: toward colloidal science and cellular adhesion applications (Adv. Funct. Mater. 18/2018), Adv. Funct. Mater. (2018).
[39] M.K. Corliss, C.K. Bok, J. Gillissen, M.G. Potroz, H. Jung, E.-L. Tan, et al., Preserving the inflated structure of lyophilized sporopollenin exine capsules with polyethylene glycol osmolyte, J. Ind. Eng. Chem. 61 (2018) 255–264.
[40] T.-F. Fan, M.G. Potroz, E.-L. Tan, M.S. Ibrahim, E. Miyako, N.-J. Cho, Species-specific biodegradation of sporopollenin-based microcapsules, Sci. Rep. 9 (1) (2019).
[41] T. Kokubo, H. Takadama, How useful is SBF in predicting in vivo bone bioactivity? Biomaterials 27 (15) (2006) 2907–2915.
[42] P.E. Jardine, F.A. Abernethy, B.H. Lomax, W.D. Gosling, W.T. Fraser, Shedding light on sporopollenin chemistry, with reference to UV reconstructions, Rev. Palaeobot. Palynol. 238 (2017) 1–6.
[43] M. Bağcıoğlu, B. Zimmermann, A. Kohler, A multiscale vibrational spectroscopic approach for identification and biochemical characterization of pollen, PLoS One 10 (9) (2015), e0137899.
[44] F. Ahlers, H. Bubert, S. Steuernage, R. Wiermann, The nature of oxygen in sporopollenin from the pollen of Typha angustifolia L, Z. Naturforsch. C 55 (3–4) (2000) 129–136.
[45] E. Domínguez, J.A. Mercado, M.A. Quesada, A. Heredia, Pollen sporopollenin: degradation and structural elucidation, Sex. Plant Reprod. 12 (3) (1999) 171–178.